Offshore transport of floodwaters following extreme storms impacts sponge health and associated microbial communities

Running title: Offshore sponge microbiomes after extreme storms

Amanda N. Shore[1*], Jordan A. Sims[1], Michael Grimes[2], Lauren I. Howe-Kerr[1], Lauren Stadler[3], Jason B. Sylvan[4], Kathryn E.F. Shamberger[4], Sarah W. Davies[5], Lory Z. Santiago-Vázquez[2], Adrienne M.S. Correa[1]

1. BioSciences, Rice University, Houston, TX, USA.

2. Biology and Biotechnology, University of Houston-Clear Lake, TX, USA.

3. Civil and Environmental Engineering, Rice University, Houston, TX, USA.

4. Oceanography, Texas A&M University, College Station, TX, USA.

5. Biology, Boston University, Boston, MA, USA.

* Corresponding author: Dr. Amanda N. Shore amanda.n.shore@gmail.com

Keywords: *Agelas clathrodes*, coral reef, flood, Flower Garden Banks National Marine Sanctuary (FGBNMS), Gulf of Mexico, Hurricane Harvey, microbial community, *Xestospongia muta*

Abstract

Terrestrial runoff can negatively impact marine ecosystems through stressors including excess nutrients, freshwater, sediments, and contaminants. Severe storms, which are increasing with global climate change, generate massive inputs of runoff over short timescales (hours to days); such runoff impacted offshore reefs in the northwest Gulf of Mexico (NW GoM) following severe storms in 2016 and 2017. Several weeks after coastal flooding from these events, NW GoM reef corals, sponges, and other benthic invertebrates experienced mortality (2016 only) and/or sub-lethal stress (both years). To assess the impact of storm-derived runoff on reef filter feeders, we characterized the microbiomes of two sponges, *Agelas clathrodes* and *Xestospongia muta*, during periods of lethal stress, sub-lethal stress, and no stress over a three-year period (2016-2018). Increased anaerobes during lethal stress indicate hypoxic conditions were associated with the 2016 mortality event. Additionally, we found evidence of wastewater contamination (based on 16S rRNA gene libraries and quantitative PCR) in sponges 185 km offshore following storms (2016 and 2017), but not during the non-flooding year (2018). We show that flooding after severe storms reaches offshore reef ecosystems and may impact offshore benthic organisms, highlighting the need for molecular and microbial time series from near- and offshore reef ecosystems, and for the continued mitigation of stormwater runoff and climate change impacts.

Importance

Stressors associated with terrestrial runoff have contributed to substantial population declines in nearshore marine ecosystems worldwide over the last three decades. It has been assumed that offshore marine ecosystems (>100 km from land) are largely unaffected by terrestrial runoff. Our findings, however, suggest that flooding events can significantly impact offshore marine organisms, based on the detection of shifted microbiomes and human pathogens in offshore sponges after extreme storm events across two separate years, and lack of detection in a non-flooding year.

INTRODUCTION

Tropical coral reef ecosystems have evolved in the context of nutrient-poor (oligotrophic) waters. Thus, when nutrient-laden (eutrophic) terrestrial runoff mixes with reef-associated waters, this can directly or indirectly stress or kill reef organisms (1–4). Terrestrial runoff exposes reef organisms to decreased salinity, and increased levels of turbidity and contaminants (e.g., microbial pathogens, chemical pollutants) (3). Terrestrial runoff can also reduce dissolved oxygen levels in reef-associated waters through several mechanisms (reviewed in reference 5). For example, excess nutrients in runoff trigger bacterial and zooplankton blooms, which draws down oxygen in the water column via respiration (5); turbidity limits the ability of phototrophs to produce oxygen (3); and hyposalinity can stratify the water column preventing reoxygenation of bottom waters (6). Terrestrial runoff can constitute a chronic stress in areas with developed coastlines or at river outflows, or an acute stress when floodwaters generated by extreme storms move offshore. Floodwaters originating in urban areas may constitute a greater threat, containing high nutrient and contaminant loads due to overflows of wastewater management systems (7, 8). Storm-associated runoff is increasingly recognized as a threat to reefs since the intensity and precipitation associated with tropical storms is increasing with climate change (9, 10).

Although various studies document the impacts of terrestrial runoff on coral reefs, few works specifically address runoff derived from floodwaters; all of these latter works focus on nearshore, shallow water reefs (11, 12). It has been assumed that offshore or deep (e.g., mesophotic) reefs are unlikely to interact with terrestrial runoff (13). For example, reefs within the Flower Garden Banks National Marine Sanctuary (FGBNMS, northwest Gulf of Mexico, Figure 1a) occur ~185 km offshore in relatively deep water (20-30 m), boast some of the highest coral cover (~55%) in the wider Caribbean (14), and have been generally presumed to be protected from land-based stressors (14). Low salinity (< 33 parts per thousand) water from terrestrial runoff has been detected within the FGB for the past several decades (15–17); however, the impact of these waters on reef ecosystem health has not been directly studied.

Since 2015, the Texas coast has experienced several flooding events related to extreme storms: Memorial Day Flood of 2015; Tax Day Flood of 2016, Hurricane Harvey in 2017, and Hurricane Imelda

in 2019. Each of these floods impacted Central Texas nearshore ecosystems, including salt marshes (18, 19) and oyster beds (20). In addition, a significant decline in surface water salinity occurred near the East Bank in the FGB following the 2015 flooding event, but it was assumed floodwaters would not impact the benthic reef ecosystem at 20-30 m depth. However, three months after Tax Day flooding in 2016, a localized mortality event occurred on a portion of the East Bank (EB) of the FGB. During the mortality event, approximately 82% of corals in a 0.06 km^2 area, experienced partial or full mortality (21), and mortality in many other benthic invertebrates, such as sponges, was also observed. Although data on abiotic conditions on the reef at East Bank during the 2016 mortality event are not available, measurements from nearby sites suggest that poor water quality from floodwaters moving offshore and low dissolved oxygen levels played a role in the mortality event (6, 22). Then, in late August of 2017, Hurricane Harvey released over one meter of rainfall over the course of six days in some areas of southeastern Texas (23). Although surface salinity was slightly depressed near the FGB following Hurricane Harvey, much of the water mass diverted southwest along the coast (24), and no mass mortality was observed on the reef (25).

Benthic reef invertebrates, such as sponges, harbor a diversity of microbial symbionts (e.g., bacteria, archaea, protists, fungi and viruses) that contribute to their health and nutrition but can be disrupted by environmental stress, including terrestrial runoff (26). This study assesses whether storm-derived coastal flooding events can perturb the microbial symbioses of offshore reef sponges. We leverage the Tax Day Flood (2016) and Hurricane Harvey (2017) as natural 'experimental treatments' applied to two sponge species (*Xestospongia muta* and *Agelas clathrodes*; Figure 1b-c) at the East Bank (EB) and West Bank (WB) of the FGB. Bacterial communities were sampled from sponges at five time points: in July 2016 (at detection of the mortality event), one month after the mortality event (August 2016), immediately after Hurricane Harvey (September 2017), one month after Hurricane Harvey (October 2017), and approximately one year following Hurricane Harvey (October 2018) (Figure 1d). No flooding occurred in southeast central Texas during 2018, and thus samples from this time point function as an 'experimental baseline'. We hypothesized that: (1) sponge-associated bacterial communities shift during flood years (relative to the non-flood year); (2) flood year bacterial communities contain genetic signatures of terrestrial-derived bacteria;

and (3) anaerobes have a higher relative abundance in July 2016, reflecting hypoxic conditions that likely occurred during the mortality event. Understanding how and when environmental stressors influence sponge-microbe associations, and the subsequent implications for sponge health and function, is important as sponges increase in abundance and in ecological importance on Caribbean reefs (27, 28).

RESULTS

Reduced surface salinity at the FGB following floods

In the vicinity of the FGB, mean surface salinity is generally variable between mid-May through mid-August (shaded grey in Figure 1d). In early spring and in fall, however, surface salinity is more consistent (~ 35 ppt). Approximately 30 days after the 2016 Tax Day Flood impacted Texas, a period of depressed mean surface salinity (relative to the mean surface salinity for a six year period: 2013-2018) was recorded from 15 May 2016 to 15 August 2016 at Texas Automated Buoy System (TABS) Real Time Ocean Observations, Buoy V. On average, surface salinity was 1.2 ppt lower than the six-year mean during this period; the most significant deviation occurred around 2 July 2016 when mean surface salinity reached a minimum of 29.1 ppt (3.2 ppt below the six-year mean). In 2017, surface salinity remained > 35 ppt until early June. TABS buoy V data are unavailable for much of June to August 2017, so it is unclear how surface salinity changed in the months preceding Hurricane Harvey. Two abrupt reductions in surface salinity (to 32.6 ppt and 32.7 ppt) were recorded near the FGB during mid-to-late September 2017 following Hurricane Harvey, before surface salinity returned to 35 ppt in October. In contrast, no significant influence of freshwater was recorded in 2018 and surface salinity remained approximately 35 ppt after mid-June.

After the 2016 mortality event was discovered at EB, opportunistic sampling of debris from dead organisms, hereafter referred to as ‘dead invertebrate tissue’, occurred on 27 July 2016; the mean surface salinity was 31.7 ppt, which was 2.1 ppt below the six-year mean for the area (Figure 1d). On this date, mean surface salinity had already been lower than the six-year mean for 44 days. Additional samples were collected on 6 August 2016, approximately four days after surface salinity had returned to 35 ppt (Figure 1d). Sampling immediately post-Hurricane Harvey on 16 September 2017 occurred when mean surface

salinity was 34.6 ppt, or 1.3 ppt lower than the six-year mean (Figure 1d). During sampling that occurred approximately one-month post-hurricane (on 21 October 2017), mean surface salinity had been > 35 ppt for 19 days prior to sampling (Figure 1d). Samples for the non-flood year were collected on 23 October 2018, which had a mean surface salinity of 35.7 ppt; surface salinity had been > 35 ppt for 94 days (Figure 1d).

Acute shifts in sponge-associated bacterial communities following flood events

Paired-end Illumina MiSeq sequencing of the V4 region of the bacterial 16S rRNA gene yielded 4,572,505 high quality sequences from samples of dead invertebrate tissue (associated with the 2016 mortality event, n=8) and two sponge species (*A. clathrodes*, n=54; *X. muta*, n=44) (Table 1, Supplemental Table S1). After removal of Mitochondrial, Chloroplast, and Unassigned reads, the total pool of bacterial sequences were assigned to 5,161 Amplicon Sequence Variants (ASVs). All samples clustered into 4 distinct groups (Figure 2), which were all significantly different from each other (ANOSIM: $p < 0.01$; Supplemental Table S2). These groups were: 1) dead invertebrate hissue (July 2016); 2) diseased sponges of both species (Aug. 2016); 3) visually healthy *A. clathrodes* (Aug. 2016, Oct. 2017, Oct. 2018); and 4) visually healthy *X. muta* (Aug. 2016, Sept. 2017, Oct. 2017, Oct. 2018). Because healthy sponges had species-specific bacterial communities (ANOSIM: Global $R = 0.688$, $p = 0.01$), subsequent analyses were conducted on each sponge species individually. Additionally, within each sponge species, there were no differences between EB and WB sites (ANOSIM: $p > 0.05$) (Supplemental Table S3), therefore, sites were grouped for subsequent analyses.

Bacterial communities of *X. muta* were shifted significantly during all collection dates associated with flood events (Aug. 2016, Sept. 2017, Oct. 2017), relative to samples collected during the same season in a no flood, baseline year (Oct. 2018) (ANOSIM: $p < 0.05$, Supplemental Table S4). Bacterial communities of *X. muta* in Aug. 2016 and Sept. 2017 showed the greatest shift (Figure 3a) and had significantly higher variability (mean pairwise dissimilarity) compared to Oct. 2018 communities (Kruskal-Wallis with Dunn's comparisons: $p < 0.001$) (Figure 3b). In Oct. 2017, *X. muta* bacterial community

structure was still significantly different than bacterial communities under ambient conditions (Oct. 2018, Supplemental Table S4). However, Oct. 2017 communities clustered more closely to Oct. 2018 than to Sept. 2017 communities (Figure 3a), and variability of bacterial communities in Oct. 2017 was similar to that in Oct. 2018 (Kruskal-Wallis with Dunn's comparisons: $p = 0.982$, Figure 3b). Bacterial communities of *X. muta* had similar levels of Shannon Diversity across time points (Kruskal-Wallis: $H = 0.747$ $p = 0.862$). However, there was a significant difference in ASV richness over time (Kruskal-Wallis: $H = 12.76$ $p = 0.005$), with communities from Aug. 2016 having higher ASV richness than communities from Oct. 2018. *X. muta* bacterial communities during Oct. 2018 of the no flood year were dominated by Chloroflexi (21.4 ±1.2%), Gammaproteobacteria (14.0 ±1.0%), Acidobacteria (13.1 ±1.4%), and Actinobacteria (10.1 ±1.2%) (Supplemental Figure S1a). DESeq2 analysis identified diverse *X. muta*-associated bacterial families whose abundance differed significantly during flooding events, as compared to Oct. 2018 (Supplemental Table S5). Clostridiaceae, Poribacteria, and SAR86 clade were all enriched in both Aug. 2016 and Sept. 2017. Clostridiaceae experienced the greatest change of any significantly abundant Family; 19.7 and 21.2 log2 fold change for Aug. 2016 and Sept. 2017, respectively. No bacterial Family was enriched or depleted across all three flood-associated collection dates (Aug. 2016, Sept. 2017, Oct. 2017).

Similar to *X. muta*-associated bacterial communities, bacterial communities of *A. clathrodes* also shifted significantly during all collection dates, relative to 'baseline' samples collected during a no flood year (Oct. 2018). *A. clathrodes* communities also differed between flooding events (Aug. 2016 vs. Oct. 2017, Figure 3c, Supplemental Table S4). Like in *X. muta*, bacterial communities in *A. clathrodes* displayed higher variability in response to the flood events (Figure 3d). *A. clathrodes* bacterial communities displayed differences in both ASV richness (Kruskal-Wallis: $H = 38.79$ $p = 0.001$) and Shannon Diversity (Kruskal-Wallis: $H = 24.16$ $p = 0.001$) across time points, with Oct. 2017 having significantly lower ASV richness and diversity. *A. clathrodes* bacterial communities during Oct. 2018 were also dominated by Chloroflexi (22.7 ±1.2%), Gammaproteobacteria (15.3 ±1.0%), Actinobacteria (15.2 ±1.6%), and Acidobacteria (13.6 ±0.6%) (Supplemental Figure S1b). DESeq2 analysis identified 27 bacterial Families were enriched in Aug. 2016 as compared to Oct. 2018; in contrast, only 8 Families were enriched in Oct. 2017 (Supplemental

Table S5). Similar to *X. muta*, in *A. clathrodes* bacterial communities, Clostridiaceae was enriched immediately following flooding events (Aug. 2016). Families with potential human and marine pathogens, Enterobacteriaceae and Vibrionaceae, were significantly enriched following flooding in Aug. 2016 (Supplemental Table S5). One Family, Stappiaceae (Class Alphaproteobacteria; Order Rhizobiales), was enriched in both Aug. 2016 and Oct. 2017 (Supplemental Table S5).

Over 300 ASVs (204 and 132 ASVs in *X. muta* and *A. clathrodes* communities, respectively) were significantly associated with flooding events as detected by Indicator Species Analysis (Indicator Value > 0.3, $p < 0.05$; Supplemental Table S6). Fifteen indicator ASVs were detected in both sponge species in Aug. 2016, and one indicator ASV was detected in both Aug. 2016 and Sept. 2017 (Table 2; Supplemental Table S6). No ASVs were significantly associated with Oct. 2017, one-month post-Hurricane Harvey, in both sponge species, and no ASVs were significantly associated with all three flooding related collection dates (Aug. 2016, Sept. 2017, and Oct. 2017). Seven ASVs classified as *Prochlorococcus* and *Synechococcus* (Phylum Cyanobacteria) were associated with flooding events, and one particular ASV, classified as Prochlorococcus, was significantly associated with both sponge species in Aug. 2016 (Supplemental Table S6). Additionally, sulfate-reducing bacteria, two ASVs classified as *Halodesulfovibrio* and two ASVs classified as *Desulfovibrio*, were associated with the Aug. 2016 flooding event in both sponge species (Table 2, Supplemental Table S6).

<u>Sponge microbiomes during the July 2016 mortality event were dominated by anaerobes</u>

Bacterial communities from visually healthy and diseased sponges sampled immediately after the mortality event were dominated by taxa classified as aerobes (mean = 26.5 ± 5.0% and range = 5.8 – 64.9%, Figure 4). However, bacterial communities from dead invertebrate tissue sampled during the mortality event had a significantly higher mean proportion of taxa classified as anaerobes (29.8 ± 5.1%), compared to bacterial communities sampled from sponges at all other time points (3.2 ± 0.4%) (Kruskal-Wallis with Dunn's multiple comparisons; $p < 0.02$, Figure 4). Within bacterial communities of dead invertebrate tissue samples, there were 19 Families at > 0.1% relative abundance. Fourteen of these Families were

characterized as obligate, facultative, or aerotolerant anaerobes, including several members of the Class Bacteroidetes, several members of the Class Clostridia, sulfate-reducers (Family Desulfovibrionaceae), and sulfur-oxidizers (Family Thiothrichaceae) (Supplemental Figure S2a). Some of the same taxa that were abundant in dead invertebrate tissue samples (July 2016), such as Flavobacteriaceae and Desulfovibrionaceae, were also abundant in diseased sponge samples (Aug. 2016) (Supplemental Figure S2b), but were absent (or were in minor taxa, < 0.1%) in visually healthy sponges.

Sponge microbiomes show signs of wastewater contamination after flooding

Bacterial ASVs classified as Family Enterobacteriaceae were recovered from the majority of samples of both sponge species. In *X. muta*, bacterial communities had low abundances (< 0.1%) of Enterobacteriaceae (Figure 5a), displaying no significant differences across dates (Kruskal-Wallis: H = 6.194, p = 0.185). However, *A. clathrodes* bacterial communities in 2016 (diseased and visually healthy samples) had a significantly higher abundance of Enterobacteriaceae (Kruskal-Wallis: H = 23.33, p = 0.001), relative to samples from this host in other years. Bacterial communities of *A. clathrodes* in Aug. 2016 displayed 8.80 (± 2.54)% and 1.45 (± 0.97)% abundance of Enterobacteriaceae for diseased and visually healthy samples, respectively, whereas in Oct. 2017 and Oct. 2018, samples had a low abundance (< 0.1%) of Enterobacteriaceae (Figure 5b). However, no ASVs classified in the Family Enterobacteriaceae were identified in Indicator Species Analysis as being significantly associated with either flooding event (Supplemental Table S6).

To test the hypothesis that FGB sponges were exposed to wastewater-derived bacteria from storm generated floodwaters, samples were screened for seven human pathogens using quantitative PCR. Diseased and visually healthy sponge samples collected in 2016 and 2017 yielded positive detection for 2 out of 7 human pathogens screened: *Escherichia coli* and *Klebsiella pneumoniae* (Figure 5c,d). No human pathogens were detected from sponges sampled during the no flood year (Figure 5c,d). In *X. muta*, *E. coli* abundance was highest in visually healthy samples from Aug. 2016, with a mean of 1.96 $x10^3$ (± 1.40 $x10^3$) gene copies per g tissue, compared to a mean of 8.96 $x10^1$ (± 8.54 $x10^1$) and 6.90 $x10^1$ (± 2.18 $x10^1$) gene

copies per g tissue for diseased samples from Aug. 2016 and visually healthy sponges from Sept. 2017, respectively (Figure 5c). However, *E. coli* was detected in only one *X. muta* sample in Sept. 2017. In *X. muta*, *K. pneumoniae* abundance was similar across groups, averaging 1.08 $x10^2$ (± 5.78 $x10^1$), 7.84 $x10^1$ (± 7.27 $x10^1$), and 1.06 $x10^2$ (± 6.74 $x10^1$) gene copies per g tissue for diseased samples from Aug. 2016, visually healthy sponges from Aug. 2016, and visually healthy sponges from Sept. 2017, respectively (Figure 5c). In *A. clathrodes*, *E. coli* was more abundant in samples from Aug. 2016, with means of 6.47 $x10^4$ (± 5.76 $x10^4$) and 2.85 $x10^4$ (± 1.79 $x10^4$) gene copies per g tissue for diseased and visually health sponges, respectively, compared to Oct. 2017, with a mean of 6.26 $x10^2$ (± 4.17 $x10^2$) gene copies per g tissue (Figure 5d). In *A. clathrodes*, *K. pneumoniae* was less abundant (> 2 orders of magnitude difference) compared to *E. coli*, displaying similar abundance across groups where it was detected, averaging 8.22 $x10^1$ (± 7.65 $x10^1$), 8.36 $x10^1$ (± 5.68 $x10^1$), and 4.61 $x10^1$ (± 3.29 $x10^1$) gene copies per g tissue for diseased samples from Aug. 2016, visually healthy sponges from Aug. 2016, and visually healthy sponges from Oct. 2017, respectively (Figure 5d). No samples tested positive for *Enterococcus* spp., *Pseudomonas aeruginosa*, *Salmonella enterica*, *Serratia marcescens*, and *Staphylococcus aureus* (data not shown).

DISCUSSION

<u>Microbiomes of offshore reef sponges are disrupted following major flooding events</u>

It has been assumed that remote benthic marine ecosystems (>100 km from land) are not significantly affected by terrestrial runoff. Our findings, however, suggest that flooding events can significantly impact offshore benthic reef organisms. Bacterial communities of both *X. muta* and *A. clathrodes* show disruptions to their community structure following flooding events in 2016 and 2017, relative to sponge bacterial communities collected during the same season in a no flood year in Oct. 2018. Furthermore, we quantified an increased relative abundance of the Enterobacteriaceae and two known human pathogens (*E. coli* and *K. pneumoniae*) in post-flood sponge samples, indicating that floodwaters of terrestrial origin can reach and interact with offshore reefs following extreme storm events.

Invasion of floodwater-derived bacteria into host tissues, invasion of seawater-derived microbes into host tissues and/or shifts in the abundance of sponge-associated taxa already present in hosts all could have contributed to shifts documented after these floods. To confirm the mechanism(s) underlying such microbial shifts in the field, robust manipulative experiments or 'before flood' environmental samples of seawater, floodwater, and benthic host tissues would be required (in addition to during and post-flood samples). It is plausible that all three mechanisms above contributed, albeit to different degrees, following each flood. For example, the presence of human pathogens in sponge-tissue indicates possible invasion of floodwater-derived bacteria into host tissues. Also, cyanobacteria were enriched over EB reefs following the 2016 Tax Day Flood, associated with higher ammonium concentrations from the terrestrially-derived floodwater (6); and *Prochlorococcus* (a free-living marine cyanobacterium in Family Cyanobiaceae) was identified as an indicator species for the Aug. 2016 flooding event. These data suggest possible invasion of seawater-derived microbes into sponge tissue. We also observed increases in Family Cyanobiaceae in *X. muta* in Aug. 2016 and Sept. 2017, which could have been driven by the proliferation of the resident sponge-associated *Synechococcus* (Family Cyanobiaceae) populations due to environmental changes. Reduced capacity of the animal host to regulate its microbiome under stress could be a contributing factor to any of these mechanisms (e.g., 29, 30). Although surface salinity decreased at the FGB following flooding events, salinity at depth (24 m) at the WB was unchanged preceding and during the Tax Day Flood event and July 2016 mortality event (19). This suggests that changes in salinity did not directly impact sponge microbial communities. Measurements for other environmental parameters associated with terrestrial runoff, such as turbidity, nutrient content, and pH, are not available for waters at depth at the FGB following these flood events.

Bacterial communities associated with the two sponge species in this study exhibited some differences in the strength and duration of their response to flood water stress, likely due to the fact that they harbor distinctive bacterial communities even under ambient conditions (e.g., in 2018). Bacterial communities associated with other sponge species have similarly exhibited variation in their resistance to some flood-associated stressors, such as elevated nutrients (31–33) and reduced salinity (34). Larger shifts

in *X. muta* bacterial communities were associated with the 2016 Tax Day Flood. In contrast, *X. muta* bacterial communities were relatively resilient following the sub-lethal stress associated with Hurricane Harvey, being more similar to baseline (Oct. 2018). Interestingly, *A. clathrodes* sponges exhibited larger shifts in its microbiota following Hurricane Harvey (sub-lethal stress) than it did following the 2016 Tax Day Flood, and *A. clathrodes* microbiomes remained disrupted in Oct 2017. Wright *et al*. (2019) similarly found that interspecific differences were the strongest driver of gene expression changes in two coral following Hurricane Harvey. Differences in host function or ability to regulate its bacterial community may explain why *X. muta* showed earlier changes (and more dispersion) in response to the 2017 flood, whereas shifts in *A. clathrodes* bacterial communities lingered.

<u>Wastewater contamination after severe flooding reaches offshore marine ecosystems</u>

The increased abundance of Enterobacteriaceae in reef sponges 185 km offshore after flooding in 2016 and, particularly, the detection of two fecal coliforms (*E. coli* and *K. pneumoniae*) during and after flood exposure strongly suggest that these reefs were exposed to wastewater contamination after severe storms. This signal of potential wastewater contamination remained one month after flooding (in Oct. 2017). Although the Family Enterobacteriaceae is ubiquitous in nature, occupying terrestrial, aquatic, and marine habitats, especially the intestine of homeothermic animals (35), members of this group are not common or abundant members of the microbiome of sponges (36, 37). It is possible that other sources of Enterobacteriaceae, such as excreted waste from reef fish and marine mammals (38) or wastewater disposal from nearby ships, explain the presence of this bacterial family across sponge samples. Additionally, other members of the Enterobacteriaceae besides those screened for via qPCR may explain the presence of Enterobacteriaceae reads in samples across all sampling dates. However, given that no human pathogens were detectable from October 2018 (no flood) samples, the most parsimonious explanation for the Enterobacteriaceae detections in this study is that FGB reefs were exposed to land-based human wastewater via terrestrial runoff following the 2016 and 2017 floods.

It is unclear whether wastewater-derived bacteria contributed to mortality at EB in July of 2016, but detection of wastewater contamination at FGB raises the question: do fecal coliforms pose health risks to offshore reefs? Human or animal wastewater contamination is linked to negative impacts on coral communities, particularly based on the input of excess nutrients, but chemical, bacterial, and pharmaceutical contamination are also potential issues (39). The wastewater-derived bacteria, *Serratia marcescens*, is a pathogen of *Acropora palmata* coral in the Caribbean (40, 41), and in Hawaii, fecal coliforms colonized coral tissues after exposure, potentially contributing to a major disease outbreak (42). There is little information on the effect of fecal coliform exposure on marine sponge health, but some sponges may be relatively tolerant, using bacterial cells as a source of nutrition (43). The surprisingly far reach of contaminated floodwaters observed here underscores the urgent need to understand how floodwaters impact the health and function of offshore reef environments. A key question to address is whether detection of *E. coli* and *K. pneumoniae* represent detection of DNA from dead wastewater-derived bacterial cells or whether living wastewater-derived bacteria are potentially interacting with sponges (and other marine life) following extreme storms. If wastewater-derived bacteria contaminating sponges are metabolically active, then we must determine how long they persist within the sponge microbiome and the extent to which these microbes impact sponge physiology and function. A better understanding of the interactions between benthic reef hosts and terrestrial-derived bacteria will support effective management and protection of offshore reef ecosystems, such as those in the FGBNMS.

Previous work has shown the utility of using sponges as monitoring and potential bioremediation tools for fecal-coliform contamination in near-shore environments (44, 45). Although *X. muta* is larger and thus likely has a higher filtration rate (46–48), *A. clathrodes* had a higher frequency of detection of *E. coli* and contained this bacterial taxa at higher abundances. Interspecific differences in the digestion of filtered material (49) may have contributed to differences in the abundance of human pathogens between these two sponge sponges. This work demonstrates that sponge species can be effective tools for monitoring wastewater contamination in offshore marine ecosystems, and that the species selected for monitoring requires consideration.

Anaerobic taxa implicate hypoxia in the 2016 mortality event at East Flower Garden Bank

The increasing potential for hypoxic conditions on reefs has recently been recognized (5, 50) yet, relatively little is known regarding how often low dissolved oxygen contributes to reef decline and over what spatiotemporal scales this occurs. Although there are no direct measurements of dissolved oxygen available from the EB at the time of the July 2016 mortality event, hypoxic conditions are thought to have contributed to the mortality observed (6). In corals, hypoxic micro-environments generated by high microbial respiration at sites of coral-algal interaction cause increased microbiome variation (community dispersion), as well as increased abundance of bacteria classified as anaerobes (51). We report a similar pattern of increased abundance of strict anaerobes in sponge microbiomes collected in July 2016. Our data support the hypothesis that low oxygen conditions, likely generated by increased microbial and/or reef respiration, contributed to the 2016 mortality event at the EB.

Some anaerobes detected in dead invertebrate tissue samples (July 2016) may be of terrestrial origin. Some Genera within the Bacteroidetes, Clostridiaceae, and Christensenallaceae Families are abundant members of mammalian gut microbiota (52, 53), and are thus potential indicators of wastewater contamination on FGBNMS reefs. However, other anaerobes and microaerophiles present in dead invertebrate samples may be marine in origin. Desulfovibrionaceae and Thiotrichaceae contain sulfate-reducing and sulfur-oxidizing bacteria, respectively (54, 55), and Genera within both Families are both commonly found in anoxic and microaerophilic layers of marine sediments (56–58). Interestingly, *Beggiatoa* (Family Thiotrichaceae) and *Desulfovibrio* (Family Desulfovibrionaceae) are both essential components of the microbial consortium that causes black band disease in corals (59). *Beggiatoa* is considered an indicator of low dissolved oxygen conditions and thick, white, filamentous mats *in situ* can be presumptively identified as this genus (60–62). White, filamentous mats were also observed during the mortality event in July 2016 (21), and thus, members of the Thiotrichaceae may be the source of the ‘white bacterial mat’ described by divers during dead invertebrate sample collection. Desulfovibrionaceae and

Thiothrichaceae together may have opportunistically contributed to the mortality initially caused by hypoxic conditions on EB in July 2016.

Comparisons of FGB sponge microbiomes to those in the wider Caribbean

This study is the first to characterize sponge-associated microbial communities from the northwest Gulf of Mexico (and the FGB), offering the opportunity for comparisons of sponge microbial communities across regions of the GoM and the Caribbean. *X. muta* associated bacterial communities at the FGB in 2018 (no storm condition) were similar between EB and WB and were dominated by Phyla also commonly reported from *X. muta* in the Florida Keys, Bahamas, and greater Caribbean (i.e. Proteobacteria, Chloroflexi, Cyanobacteria, Poribacteria, and to a lesser extent, Acidobacteria, Actinobacteria, and Crenarchaeota (63–68). These previous studies report regional differences due to changes in relative abundance of these shared Phyla (63, 67). *X. muta* bacterial communities from the FGB may also be regionally distinct, in particular containing a high abundance of Crenarchaeota archaea (~10%) compared to what has been reported from other regions (<5%) (69). Ammonia oxidizing Archaea, such as Nitrosomopumilaceae, play an important role in nitrogen cycling in *X. muta* (70). Ammonia-oxidizing archaea are outcompeted in environments with higher levels of ammonium (71), so the greater abundance of Nitrosomopumilaceae likely reflects the oligotrophic environment of the offshore FGB reefs during no storm conditions.

This study is also the first to describe bacterial communities associated with *A. clathrodes* using next-generation sequencing technology. Bacterial communities of *A. clathrodes* at the FGB contained Phyla (i.e. Proteobacteria, Firmicutes, Actinobacteria, Chloroflexi, Crenarchaeota) also present in other *Agelas spp.* from the Florida Keys, Belize, and Central Amazon Shelf (65, 72–74). However, higher abundances of Archaea, especially Euryarchaeota and Crenarchaeota, and Firmicutes were found in other *Agelas* spp. (72, 73). Diseased sponges (both *A. clathrodes* and *X. mut*a) sampled after the 2016 mortality event were dominated by Alphaproteobacteria, especially Rhodobacteraceae. Alphaproteobacteria were also enriched

in sponges affected by *Agelas* Wasting Syndrome (72), suggesting that this group of bacteria could play a role in pathogenesis and/or serve as a biomarker of disease risk for FGB sponge communities.

Mitigating the Impacts of Future Storms on Offshore Reefs

This study demonstrates that transport of floodwaters following extreme storms can contribute to shifts in the microbiomes of benthic reef organisms 185 km offshore, promoting bacterial communities that are more variable. Detection of bacteria typically associated with wastewater within these sponge samples illustrates that marine-terrestrial interactions, and thus, the potential impacts of human land and waste management practices, extend far beyond the shoreline. The GoM is regularly impacted by hurricanes, and thus marine communities in the region have evolved in a disturbance regime that includes bursts of storm-generated terrestrial runoff. However, the ongoing expansion of impermeable surfaces (e.g., concrete, pavement) in Texas and other coastal areas, as well as changing extreme storm patterns (e.g., slower moving hurricanes with greater precipitation) are increasing the frequency and intensity of floodwater influx into marine environments.

This study of the potential impacts of the 2016 and 2017 floods was catalyzed because a mortality event affected the East Bank following the Tax Day Flood. We hypothesize that flood waters associated with other recent extreme storm events (e.g., 2015 Memorial Day Flood, flooding generated by Hurricane Imelda in September 2019) in the region likely also caused sub-lethal stress at the FGB. However, targeted sampling of FGB did not occur following these storms. Our findings clearly demonstrate the urgent need for: 1) continued mitigation of stormwater runoff and climate change impacts; and 2) establishment of surface and benthic microbial and water quality time series for near- and offshore reef using standardized protocols. This latter program will ideally generate baseline data on the gene expression and microbiomes of key benthic reef taxa under normal conditions, providing critical context (75) in which to detect and mitigate floodwater-derived stress on reefs in order to understand their impact on benthic invertebrate physiology and reef ecosystem functions.

EXPERIMENTAL PROCEDURES

Pelagic water properties during sample collection periods

The Flower Garden Banks National Marine Sanctuary (FGBNMS, northwest Gulf of Mexico) is currently comprised of three banks: East Bank (EB), Stetson Bank and West Bank (WB) (Figure 1a). To characterize local surface salinity (sensor depth of 2 m) in parts per thousand (ppt) representative for the FGB before, during, and after each sampling period, water property data collected each half hour for April - October for the years 2013 - 2018 were downloaded from the Texas Automated Buoy System Real Time Ocean Observations, Buoy V archives (http://tabs.gerg.tamu.edu). Buoy V (27° 53.7960'N, 93° 35.8380'W) is located approximately 3 km from EB and 25 km from WB. Data were filtered to remove all timepoints containing no data and to exclude outlier data (i.e., measurements where salinity abruptly changed to <1 ppt or >70 ppt from 35 ppt). Data were not available (due to instrumentation failure) between the dates of 6 June 2017 through 30 August 2017. The remaining data were then plotted using the ggplot2 package version 3.2.1 using code from https://github.com/rachelwright8/TagSeq_FGB_HurricaneHarvey. Data were summarized to determine means (black line) and daily ranges (grey shading) for April to October over the six-year period. To assess the lags between continental flooding (associated with an extreme storm) and changes in water quality at the FGB, daily salinity mean and range data for April to October of individual years 2015, 2016, 2017 and 2018 (red lines) were overlaid on surface salinity averages for the six-year summary data. Daily means for each sponge sampling date were also calculated and plotted on top of the six-year summary data with colored icons. (Figure 1d). For sampling campaigns that spanned more than one day, only the first day of sampling was plotted (the maximum length of a sampling campaign was 5 days).

Sponge Sample Collections

Samples were collected at five timepoints spanning 2016-2018 from two locations within the FGBNMS; East Bank (27° 52'54.84”, 93° 37'41.84") and West Bank (27°54'28.8", 93°36'0.72", Figure 1a, Table 1). Samples from July 2016 were samples of dead invertebrate tissue collected opportunistically on

the day that the EB mortality event was discovered; sampling capabilities at this time point were extremely limited in terms of available sterile collection materials and dive time, relative to subsequent sample time points. Thus, the July 2016 dead invertebrate tissue samples are a composite representation of the organic mat that had formed on the tops of dying sponges, corals, and other organisms including brittle stars and urchins (Supplemental Table S5). Representative photos of dead invertebrates during the July 2016 mortality event are presented in Johnston *et al.*, (2018). At all other sampling timepoints, fragments were collected from individual *A. clathrodes* and *X. muta* sponges. The same individual sponges were not repeatedly sampled across timepoints due to time constraints in available ship and dive time. In August 2016, samples were collected from 'diseased sponges' that were exhibiting progressive tissue loss, as well as from visually healthy sponges. For all other timepoints, samples were collected from visually healthy sponges as diseased sponges were not observed. In total, 109 samples, collected from depths ranging 18 - 27 m, are analyzed in this study (individual sample metadata provided in Supplemental Table S1). Samples were clipped from sponge individuals using health status and species-specific cutting shears that were wiped clean between samples. Each sample was placed in an individual sterile bag for transport to the surface. Once topside, each sample was immediately transferred to liquid nitrogen and stored at -20°C until further processing.

Bacterial Community Analysis

DNA was extracted from 250 mg of sponge sample using the Nucleospin Soil DNA extraction kit (Takara Bio); whereas DNA from dead invertebrate tissue samples was extracted using the DNeasy PowerSoil DNA extraction kit (QIAGEN). DNA from dead invertebrate tissue samples collected during the July 2016 mortality event was submitted to the Georgia Genomics Bioinformatic Core for sequencing; all other samples were sequenced at the Baylor College of Medicine's Alkek Center for Metagenomics & Microbiome Research. High-throughput sequencing of the V4 hypervariable region of the 16S gene was conducted with 515f: 5' GTGYCAGCMGCCGCGGTAA 3' and 806rb: 5'

GGACTACNVGGGTWTCTAAT 3' primers (76) using the Illumina Mi-Seq (Paired-end 2x 250 read) platform.

Sequence analysis was conducted using QIIME2 v. 2019.10 pipeline (77). Pair-end, demultiplexed reads were quality filtered, trimmed of poor-quality bases, de-replicated, chimera filtered, pair merged, and identified as amplicon sequence variants (ASVs) using the DADA2 plug-in (78). Taxonomy was assigned by training a naïve-Bayes classifier on the V4 region of the 16S gene in the SILVA version 138 database (79) using the feature-classifier plugin (80) to match the primers used. Low abundance sequences (< 10 occurrences over all samples) and non-prokaryotic ASVs (i.e., mitochondria, chloroplast, eukaryote, and unknown sequences) were then removed. Rarefied ASV tables (rarefied to 12,000 reads per sample) were used to calculate alpha diversity metrics and to conduct beta diversity analyses using weighted UniFrac distance matrices. Bacterial genera were also categorized by oxygen requirement using descriptions in Bergey's Manual of Bacteriology (35), as well as information from two online resources: the Integrated Microbial Genomes database (IMG; https://img.jgi.doe.gov/) and the eLibrary of Microbial Systematics and Genomics (eLMG; https://www.biosino.org/elmsg/index). This approach has been successfully done in previous studies (81–85). Bacterial Genera that have multiple oxygen requirements were classified as "Various", and taxonomic assignments that were not resolved to the Genus level (at 80% confidence) were listed as "Unclassified".

Quantitative PCR for human pathogens associated with Hurricane Harvey-derived floodwaters

Species-specific functional genes were chosen as biomarkers to detect and quantify fecal indicator bacteria (*Escherichia coli* and *Enterococcus spp.*), putative pathogenic bacteria in the Family Enterobacteriaceae (*Klebsiella pneumoniae*, *Serratia marcescens*, and *Salmonella enterica*), and other putative pathogenic bacteria (*Pseudomonas aeruginosa* and *Staphylococcus aureus*, Supplemental Table S7). These bacterial species were targeted because they were identified in qPCR screening and in high-throughput sequencing of terrestrial floodwater and sediment samples collected immediately following Hurricane Harvey (86).

Target gene amplicons were used to establish the standard curve between the threshold cycle (Ct) value and log10 (gene copies) for each pathogenic bacterium individually. To generate amplicons for target gene quantitation, genomic DNA of pure cultures of each bacterial strain was extracted using DNeasy PowerSoil Kit (Qiagen) and target genes were amplified by conventional PCR (50 µL reactions) with EmeraldAmp GT PCR Master Mix (Takara Bio, thermocycler conditions listed in Supplemental Table S7). Five µL of each PCR product was visualized via gel electrophoresis to confirm amplification, and the remaining PCR product was cleaned using GeneJET PCR Purification Kit (ThermoScientific). Amplicon concentration was quantified using a Qubit 3 Fluorometer (Invitrogen) with dsDNA Broad Range Assay (Invitrogen), amplicon quality was assessed using a NanoDrop One (Thermo Scientific), and amplicon sequences were confirmed via Sanger sequencing. Verified amplicons were then serially diluted to create a set of standards of known concentrations, calculated by the Thermo Fisher DNA Copy Number Calculator (https://www.thermofisher.com/us/en/home/brands/thermo-scientific/molecular-biology/molecular-biology-learning-center/molecular-biology-resource-library/thermo-scientific-web-tools/dna-copy-number-calculator.html). Each standard curve was established by linear regression of the threshold cycle (C_T) values versus the log-normal (10 base) abundance of gene copies (10^8, 10^7, 10^6, 10^5, 10^4, 10^3, 10^2) from technical triplicates. R^2 values of least square fit ranged from 0.995-0.999 for all the standard curves. The qPCR amplification efficiency for all the biomarkers ranged from 92 - 105%, calculated by plotting average C_T vs amplicon concentration (copies/µL) on a $\log_{10}$ scale. To assess gene copy number in a given sample, C_T values of samples were compared to a prepared standard curve that was included in triplicate with each qPCR run. Calculated copy number was normalized to g of wet sponge tissue. The limit of quantification ranged from 20 - 100 gene copies.

Quantitative PCR reaction mix consisted of 5 µL 2x Power SYBR Green Master Mix (Applied Biosystems), 1 µL DNA, 1.3 µL of each primer (10 µmol stock), and molecular-grade water, for a final volume of 10 µL. Primer specifications and thermocycler conditions for each pathogen are listed in Supplemental Table S2. All samples were run in triplicate on a QuantStudio 3 Real-Time PCR System (ThermoScientific) and were screened for all seven pathogens (Supplemental Table S7). Negative controls

(no template) were run in triplicate for each qPCR experiment to monitor for potential contamination. The temperature profile for SYBR Green qPCR involved 95°C for 10 min, 45 cycles of 95°C for 15 sec and annealing/extension temperature of 54 – 65°C for 1 min. Melt curve analysis was conducted after PCR completion to ensure nonspecific PCR products were not generated. Specificity of each qPCR assay was confirmed by testing for amplification in all pathogen strains used in this study as well as in four environmental isolates (*Vibrio* sp., *Alteromonas* sp., *Pseudoalteromonas* sp., and *Shewanella* sp.) previously cultured from FGB coral. No non-target strains amplified below a threshold cycle (C_T) of 30. Amplifications were considered to be positive if all three replicates amplified at a threshold cycle (C_T) less than 28 and melt curve analysis showed similar patterns to the standard.

Statistics

The weighted UniFrac distance matrix was used to calculate beta-diversity and to assess within group dispersion in bacterial communities and to construct Principle Coordinates Analysis (PCoA) plots to visualize differences in bacterial community structure between groups. PCoA was conducted for all samples (both sponge species), as well as for healthy samples of each species individually. Pairwise Analysis of Similarities (ANOSIM), conducted with 999 permutations, was used to test for significant differences in bacterial communities among categorical variables including species, health state, site, and collection date. To assess differences in bacterial abundance at the Family level, the unrarefied ASV table for each species was first summarized to Family level using tax_glom in phyloseq (v1.30.0). A negative binomial model was then fitted with the R package DESeq2 (v1.26.0) and Wald tests were used to test for differences in taxon abundance within each comparison of sampling time versus the ‘control’ sampling time (October 2018). Benjamini-Hochberg FDR tests were used to account for multiple comparisons, and Families with p-values less than 0.05 were identified as significantly differentially abundant. Indicator species analysis was performed to test the association between bacterial community and collection date, using indicspecies (v1.7.9) package in R. Significance was assessed with 9999 permutations, and ASVs with p-values less than 0.05 selected. Kruskal-Wallis non-parametric test was used to compare results such as alpha diversity

metrics, beta-diversity metrics, and quantified bacterial abundances among collection dates (within each sponge species). All data are represented as mean (± SEM), unless otherwise stated.

Data Availability

The raw sequence data files were submitted to the NCBI Sequence Read Archive under accession number SRP248232. Data files including Sample Metadata, ASV Table, ASV Taxonomy Assignment, and R script for DESeq and Indicator Species analysis are available on FigShare at https://figshare.com/account/home#/projects/82841.

Acknowledgements

This work was funded by NSF awards OCE-1800914 to AC, OCE-1800905 to LSV, OCE-1800904 to SD, OCE-1800913 to KEFS and JBS, as well as a Rice University Faculty Initiative award to AC and LS, and a NAS Gulf Research Program Early Career Fellowship and Rice University start-up funds to AC. AS was supported by a Rice Academy Postdoctoral Fellowship and Rice University start-up funds (to AC). We thank Marissa Nuttall, John Embesi and James MacMillan (NOAA), Jake Emmert and Kaitlin Buhler (Moody Gardens), and Ryan Eckert (Florida Atlantic University) for field and logistical support. We are grateful to Emma Hickerson for facilitating collection permits. We also acknowledge the following members of the science party during sampling cruises: Carsten Grupstra, Jennifer Drummond, Kelsey Sanders, and Anna Knochel (Rice University), Shawn Doyle (TAMU). We also acknowledge Rachel Wright for the code used to retrieve and plot TABS Buoy V data. 2016 samples were collected under FGBNMS-2014-001; 2017 and 2018 samples were collected under FGBNMS-2017-012 to AC. July 2016, August 2016 and September 2017 samples were collected on the R/V Manta, whereas October 2017 and October 2018 samples were collected aboard the R/V Point Sur. We express our sincere gratitude to the crews of these vessels, as well as members of the NOAA FGBNMS office and Moody Gardens Aquarium. All authors declare no conflict of interest.

REFERENCES

1. Kerswell AP, Jones RJ. 2003. Effects of hypo-osmosis on the coral *Stylophora pistillata*: nature and cause of 'low-salinity bleaching.' Mar Ecol Prog Ser 253:145–154.
2. Humphrey C, Weber M, Lott C, Cooper T, Fabricius K. 2008. Effects of suspended sediments, dissolved inorganic nutrients and salinity on fertilisation and embryo development in the coral *Acropora millepora* (Ehrenberg, 1834). Coral Reefs 27:837–850.
3. Fabricius KE. 2005. Effects of terrestrial runoff on the ecology of corals and coral reefs: Review and synthesis. Mar Pollut Bull 50:125–146.
4. Knight PA, Fell PE. 1987. Low salinity induces reversible tissue regression in the estuarine sponge *Microciona prolifera* (Ellis & Solander). J Exp Mar Bio Ecol 107:253–261.
5. Nelson HR, Altieri AH. 2019. Oxygen: the universal currency on coral reefs. Coral Reefs 38:177–198.
6. Kealoha AK, Doyle SM, Shamberger KEF, Sylvan JB, Hetland RD, DiMarco SF. 2020. Localized hypoxia may have caused coral reef mortality at the Flower Garden Banks. Coral Reefs 39:119–132.
7. Chen S, Lu YH, Dash P, Das P, Li J, Capps K, Majidzadeh H, Elliott M. 2019. Hurricane pulses: Small watershed exports of dissolved nutrients and organic matter during large storms in the Southeastern USA. Sci Total Environ 689:232–244.
8. Humphrey C, Iverson G, Skibiel C, Sanderford C, Blackmon J. 2019. Geochemistry of flood waters from the tar river, North Carolina associated with Hurricane Matthew. Resources 8:1–12.
9. Knutson TR, McBride JL, Chan J, Emanuel K, Holland G, Landsea C, Held I, Kossin JP, Srivastava AK, Sugi M. 2010. Tropical cyclones and climate change. Nat Geosci. Nature Publishing Group.
10. Emanuel K. 2017. Assessing the present and future probability of Hurricane Harvey's rainfall. Proc Natl Acad Sci U S A 114:12681–12684.
11. Ostrander CE, McManus MA, DeCarlo EH, Mackenzie FT. 2008. Temporal and spatial variability

of freshwater plumes in a semienclosed estuarine-bay system. Estuaries and Coasts 31:192–203.

12. Lapointe BE, Langton R, Bedford BJ, Potts AC, Day O, Hu C. 2010. Land-based nutrient enrichment of the Buccoo Reef Complex and fringing coral reefs of Tobago, West Indies. Mar Pollut Bull 60:334–343.

13. Szmant AM. 2002. Nutrient enrichment on coral reefs: Is it a major cause of coral reef decline? Estuaries 25:743–766.

14. Johnston MA, Embesi JA, Eckert RJ, Nuttall MF, Hickerson EL, Schmahl GP. 2016. Persistence of coral assemblages at East and West Flower Garden Banks, Gulf of Mexico. Coral Reefs 35:821–826.

15. Kealoha AK. 2019. Coral Reef Ecosystem Health in Response to Climate Change and Environmental Stressors. Texas A&M University, College Station.

16. Dodge RE, Lang JC. 1983. Environmental correlates of hermatypic coral (*Montastrea annularis*) growth on the East Flower Gardens Bank, northwest Gulf of Mexico. Limnol Oceanogr 28:228–240.

17. Deslarzes K, Lugo-Fernandez A. 2007. Influence of Terrigenous Runoff on Offshore Coral Reefs: An Example from the Flower Garden Banks, Gulf of Mexico, p. 126–160. *In* Aronson, RB (ed.), Geological Approaches to Coral Reef Ecology. Springer, New York, NY.

18. Congdon VM, Bonsell C, Cuddy MR, Dunton KH. 2019. In the wake of a major hurricane: Differential effects on early vs. late successional seagrass species. Limnol Oceanogr Lett 4:155–163.

19. Oakley JW, Guillen GJ. 2019. Impact of Hurricane Harvey on Galveston Bay Saltmarsh Nekton Communities. Estuaries and Coasts.

20. Kiaghadi A, Rifai HS. 2019. Physical, Chemical, and Microbial Quality of Floodwaters in Houston Following Hurricane Harvey. Environ Sci Technol 53:4832–4840.

21. Johnston MA, Nuttall MF, Eckert RJ, Blakeway RD, Sterne TK, Hickerson EL, Schmahl GP, Lee MT, MacMillan J, Embesi JA. 2019. Localized coral reef mortality event at East Flower Garden

Bank, Gulf of Mexico. Bull Mar Sci 95:239–250.

22. Le Hénaff M, Muller-Karger FE, Kourafalou VH, Otis D, Johnson KA, McEachron L, Kang HS. 2019. Coral mortality event in the Flower Garden Banks of the Gulf of Mexico in July 2016: Local hypoxia due to cross-shelf transport of coastal flood waters? Cont Shelf Res 190:103988.

23. Blake ES, Zelinsky DA. 2018. National Hurricane Center Tropical Cyclone Report Hurricane Harvey.

24. Roffer MA, Gawlikowski G, Upton M. 2018. Monitoring of the Hurricane Harvey Plume in the Gulf of Mexico. West Melbourne, FL 32904.

25. Wright RM, Correa AMS, Quigley LA, Santiago-Vázquez LZ, Shamberger KEF, Davies SW. 2019. Gene Expression of Endangered Coral (*Orbicella* spp.) in Flower Garden Banks National Marine Sanctuary After Hurricane Harvey. Front Mar Sci 6:672.

26. Slaby BM, Franke A, Rix L, Pita L, Bayer K, Jahn MT, Hentschel U. 2019. Marine Sponge Holobionts in Health and Disease, p. 81–104. *In* Symbiotic Microbiomes of Coral Reefs Sponges and Corals. Springer Netherlands.

27. Bell JJ, Davy SK, Jones T, Taylor MW, Webster NS. 2013. Could some coral reefs become sponge reefs as our climate changes? Glob Chang Biol 19:2613–2624.

28. Pawlik JR, McMurray SE. 2020. The Emerging Ecological and Biogeochemical Importance of Sponges on Coral Reefs. Ann Rev Mar Sci 12:315–337.

29. Zaneveld JR, McMinds R, Thurber RV. 2017. Stress and stability: Applying the Anna Karenina principle to animal microbiomes. Nat Microbiol 2:17121.

30. Pita L, Rix L, Slaby BM, Franke A, Hentschel U. 2018. The sponge holobiont in a changing ocean: from microbes to ecosystems. Microbiome 6:46.

31. Simister R, Taylor MW, Tsai P, Webster N. 2012. Sponge-Microbe Associations Survive High Nutrients and Temperatures. PLoS One 7:e52220.

32. Luter HM, Gibb K, Webster NS. 2014. Eutrophication has no short-term effect on the *Cymbastela stipitata* holobiont. Front Microbiol 5:216.

33. Baquiran JIP, Conaco C. 2018. Sponge-microbe partnerships are stable under eutrophication pressure from mariculture. Mar Pollut Bull 136:125–134.

34. Glasl B, Smith CE, Bourne DG, Webster NS. 2018. Exploring the diversity-stability paradigm using sponge microbial communities. Sci Rep 8:1–9.

35. Whitman WB. 2015. Bergey's manual of systematics of archaea and bacteria. Wiley, Hoboken, NJ.

36. Moitinho-Silva L, Nielsen S, Amir A, Gonzalez A, Ackermann GL, Cerrano C, Astudillo-Garcia C, Easson C, Sipkema D, Liu F, Steinert G, Kotoulas G, McCormack GP, Feng G, Bell JJ, Vicente J, Björk JR, Montoya JM, Olson JB, Reveillaud J, Steindler L, Pineda MC, Marra M V., Ilan M, Taylor MW, Polymenakou P, Erwin PM, Schupp PJ, Simister RL, Knight R, Thacker RW, Costa R, Hill RT, Lopez-Legentil S, Dailianis T, Ravasi T, Hentschel U, Li Z, Webster NS, Thomas T. 2017. The sponge microbiome project. Gigascience 6:1–7.

37. Cleary DFR, Swierts T, Coelho FJRC, Polónia ARM, Huang YM, Ferreira MRS, Putchakarn S, Carvalheiro L, van der Ent E, Ueng JP, Gomes NCM, de Voogd NJ. 2019. The sponge microbiome within the greater coral reef microbial metacommunity. Nat Commun 10:1–12.

38. Wallace CC, Yund PO, Ford TE, Matassa KA, Bass AL. 2013. Increase in antimicrobial resistance in bacteria isolated from stranded marine mammals of the Northwest Atlantic. Ecohealth 10:201–210.

39. Wear SL, Thurber RV. 2015. Sewage pollution: mitigation is key for coral reef stewardship. Ann N Y Acad Sci 1355:15–30.

40. Sutherland KP, Porter JW, Turner JW, Thomas BJ, Looney EE, Luna TP, Meyers MK, Futch JC, Lipp EK. 2010. Human sewage identified as likely source of white pox disease of the threatened Caribbean elkhorn coral, *Acropora palmata*. Environ Microbiol 12:1122–1131.

41. Sutherland KP, Shaban S, Joyner JL, Porter JW, Lipp EK. 2011. Human pathogen shown to cause disease in the threatened eklhorn coral *Acropora palmata*. PLoS One 6.

42. Beurmann S, Ushijima B, Videau P, Svoboda CM, Chatterjee A, Aeby GS, Callahan SM. 2018.

Dynamics of acute montipora white syndrome: Bacterial communities of healthy and diseased *M. capitata* colonies during and after a disease outbreak. Microbiol (United Kingdom) 164:1240–1253.

43. Chaves-Fonnegra A, Zea S, Gómez ML. 2007. Abundance of the excavating sponge *Cliona delitrix* in relation to sewage discharge at San Andrés Island, SW Caribbean, Colombia. Bol Investig Mar y Costeras 36:63–78.

44. Longo C, Corriero G, Licciano M, Stabili L. 2010. Bacterial accumulation by the Demospongiae *Hymeniacidon perlevis*: A tool for the bioremediation of polluted seawater. Mar Pollut Bull 60:1182–1187.

45. Maldonado M, Zhang X, Cao X, Xue L, Cao H, Zhang W. 2010. Selective feeding by sponges on pathogenic microbes: A reassessment of potential for abatement of microbial pollution. Mar Ecol Prog Ser 403:75–89.

46. Morganti TM, Ribes M, Yahel G, Coma R. 2019. Size Is the Major Determinant of Pumping Rates in Marine Sponges. Front Physiol 10.

47. McMurray SE, Blum JE, Pawlik JR. 2008. Redwood of the reef: Growth and age of the giant barrel sponge *Xestospongia muta* in the Florida Keys. Mar Biol 155:159–171.

48. Parra-velandia FJ, Zea S, Soest RWMVS. 2014. Reef sponges of the genus *Agelas* (Porifera: Demospongiae) from the Greater Caribbean. Zootaxa 3794:301–343.

49. Lynch TC, Phlips EJ. 2000. Filtration of the bloom-forming cyanobacteria *Synechococcus* by three sponge species from Florida Bay, U.S.A. Bull Mar Sci 67:923–936.

50. Hughes DJ, Alderdice R, Cooney C, Kühl M, Pernice M, Voolstra CR, Suggett DJ. 2020. Coral reef survival under accelerating ocean deoxygenation. Nat Clim Chang 10:1–12.

51. Barott KL, Rodriguez-Mueller B, Youle M, Marhaver KL, Vermeij MJA, Smith JE, Rohwer FL. 2012. Microbial to reef scale interactions between the reef-building coral *Montastraea annularis* and benthic algae. Proc R Soc B Biol Sci 279:1655–1664.

52. Waters JL, Ley RE. 2019. The human gut bacteria Christensenellaceae are widespread, heritable,

and associated with health. BMC Biol 17:1–11.

53. Arumugam M, Raes J, Pelletier E, Le Paslier D, Yamada T, Mende DR, Fernandes GR, Tap J, Bruls T, Batto JM, Bertalan M, Borruel N, Casellas F, Fernandez L, Gautier L, Hansen T, Hattori M, Hayashi T, Kleerebezem M, Kurokawa K, Leclerc M, Levenez F, Manichanh C, Nielsen HB, Nielsen T, Pons N, Poulain J, Qin J, Sicheritz-Ponten T, Tims S, Torrents D, Ugarte E, Zoetendal EG, Wang J, Guarner F, Pedersen O, De Vos WM, Brunak S, Doré J, Weissenbach J, Ehrlich SD, Bork P. 2011. Enterotypes of the human gut microbiome. Nature 473:174–180.

54. Castro H F, Williams N H, Ogram A. 2000. Phylogeny of sulfate-reducing bacteria. FEMS Microbiol Ecol 31:1–9.

55. Garrity GM, Bell JA, Lilburn T. 2015. Thiotrichaceae fam. nov., p. . *In* Whitman, WB, Rainey, F, Kämpfer, P, Trujillo, M, Chun, J, DeVos, P, Dedysh, S, Hedlund, B (eds.), Bergey's Manual of Systematics of Archaea and Bacteria. John Wiley & Sons, Inc.

56. Postgate JR, Campbell LL. 1966. Classification of *Desulfovibrio species*, the nonsporulating sulfate-reducing bacteria. Bacteriol Rev 30:732–738.

57. Zouch H, Karray F, Armougom F, Chifflet S, Hirschler-Réa A, Kharrat H, Kamoun L, Hania W Ben, Ollivier B, Sayadi S, Quéméneur M. 2017. Microbial diversity in sulfate-reducing marine sediment enrichment cultures associated with anaerobic biotransformation of coastal stockpiled phosphogypsum (Sfax, Tunisia). Front Microbiol 8:1–11.

58. Mußmann M, Schulz HN, Strotmann B, Kjær T, Nielsen LP, Rosselló-Mora RA, Amann RI, Jørgensen BB. 2003. Phylogeny and distribution of nitrate-storing *Beggiatoa* spp. in coastal marine sediments. Environ Microbiol 5:523–533.

59. Sato Y, Civiello M, Bell SC, Willis BL, Bourne DG. 2016. Integrated approach to understanding the onset and pathogenesis of black band disease in corals. Environ Microbiol 18:752–765.

60. Rosenberg R, Diaz RJ. 1993. Sulfur bacteria (*Beggiatoa* spp.) mats indicate hypoxic conditions in the Inner Stockholm Archipelago. Ambio 22:32–36.

61. Rabalais NN, Harper DE, Turner RE. 2001. Responses of nekton and demersal and benthic fauna

to decreasing oxygen concentrations, p. 115–128. *In* Coastal Hypoxia: Consequences for Living Resources and Ecosystem Coastal and Estuarine Studies.

62. Altieri AH, Harrison SB, Seemann J, Collin R, Diaz RJ, Knowlton N. 2017. Tropical dead zones and mass mortalities on coral reefs. Proc Natl Acad Sci U S A 114:3660–3665.

63. Fiore CL, Labrie M, Jarett JK, Lesser MP. 2015. Transcriptional activity of the giant barrel sponge, *Xestospongia muta* Holobiont: Molecular evidence for metabolic interchange. Front Microbiol 6.

64. Montalvo NF, Davis J, Vicente J, Pittiglio R, Ravel J, Hill RT. 2014. Integration of culture-based and molecular analysis of a complex sponge-associated bacterial community. PLoS One 9:1–8.

65. Olson JB, Gao X. 2013. Characterizing the bacterial associates of three Caribbean sponges along a gradient from shallow to mesophotic depths. FEMS Microbiol Ecol 85:74–84.

66. Schmitt S, Tsai P, Bell J, Fromont J, Ilan M, Lindquist N, Perez T, Rodrigo A, Schupp PJ, Vacelet J, Webster N, Hentschel U, Taylor MW. 2012. Assessing the complex sponge microbiota: Core, variable and species-specific bacterial communities in marine sponges. ISME J 6:564–576.

67. Morrow KM, Fiore CL, Lesser MP. 2016. Environmental drivers of microbial community shifts in the giant barrel sponge, *Xestospongia muta*, over a shallow to mesophotic depth gradient. Environ Microbiol 18:2025–2038.

68. Villegas-Plazas M, Wos-Oxley ML, Sanchez JA, Pieper DH, Thomas OP, Junca H. 2019. Variations in Microbial Diversity and Metabolite Profiles of the Tropical Marine Sponge *Xestospongia muta* with Season and Depth. Microb Ecol 78:243–256.

69. Fiore CL, Jarett JK, Lesser MP. 2013. Symbiotic prokaryotic communities from different populations of the giant barrel sponge, Xestospongia muta. Microbiologyopen 2:938–952.

70. López-Legentil S, Erwin PM, Pawlik JR, Song B. 2010. Effects of Sponge Bleaching on Ammonia-Oxidizing Archaea: Distribution and Relative Expression of Ammonia Monooxygenase Genes Associated with the Barrel Sponge Xestospongia muta. Microb Ecol 60:561–571.

71. Erguder TH, Boon N, Wittebolle L, Marzorati M, Verstraete W. 2009. Environmental factors

shaping the ecological niches of ammonia-oxidizing archaea. FEMS Microbiol Rev 33:855–869.

72. Deignan LK, Pawlik JR, Erwin PM. 2018. *Agelas* Wasting Syndrome Alters Prokaryotic Symbiont Communities of the Caribbean Brown Tube Sponge, *Agelas tubulata*. Microb Ecol 76:459–466.

73. Rua CPJ, de Oliveira LS, Froes A, Tschoeke DA, Soares AC, Leomil L, Gregoracci GB, Coutinho R, Hajdu E, Thompson CC, Berlinck RGS, Thompson FL. 2018. Microbial and Functional Biodiversity Patterns in Sponges that Accumulate Bromopyrrole Alkaloids Suggest Horizontal Gene Transfer of Halogenase Genes. Microb Ecol 76:825–838.

74. Gantt SE, McMurray SE, Stubler AD, Finelli CM, Pawlik JR, Erwin PM. 2019. Testing the relationship between microbiome composition and flux of carbon and nutrients in Caribbean coral reef sponges. Microbiome 7:1–13.

75. Glasl B, Bourne DG, Frade PR, Webster NS. 2018. Establishing microbial baselines to identify indicators of coral reef health. Microbiol Aust 39:42–46.

76. Apprill A, Mcnally S, Parsons R, Weber L. 2015. Minor revision to V4 region SSU rRNA 806R gene primer greatly increases detection of SAR11 bacterioplankton. Aquat Microb Ecol 75:129–137.

77. Bolyen E, Rideout JR, Dillon MR, Bokulich NA, Abnet CC, Al-Ghalith GA, Alexander H, Alm EJ, Arumugam M, Asnicar F, Bai Y, Bisanz JE, Bittinger K, Brejnrod A, Brislawn CJ, Brown CT, Callahan BJ, Caraballo-Rodríguez AM, Chase J, Cope EK, Da Silva R, Diener C, Dorrestein PC, Douglas GM, Durall DM, Duvallet C, Edwardson CF, Ernst M, Estaki M, Fouquier J, Gauglitz JM, Gibbons SM, Gibson DL, Gonzalez A, Gorlick K, Guo J, Hillmann B, Holmes S, Holste H, Huttenhower C, Huttley GA, Janssen S, Jarmusch AK, Jiang L, Kaehler BD, Kang K Bin, Keefe CR, Keim P, Kelley ST, Knights D, Koester I, Kosciolek T, Kreps J, Langille MGI, Lee J, Ley R, Liu YX, Loftfield E, Lozupone C, Maher M, Marotz C, Martin BD, McDonald D, McIver LJ, Melnik A V., Metcalf JL, Morgan SC, Morton JT, Naimey AT, Navas-Molina JA, Nothias LF, Orchanian SB, Pearson T, Peoples SL, Petras D, Preuss ML, Pruesse E, Rasmussen LB, Rivers A, Robeson MS, Rosenthal P, Segata N, Shaffer M, Shiffer A, Sinha R, Song SJ, Spear JR, Swafford

AD, Thompson LR, Torres PJ, Trinh P, Tripathi A, Turnbaugh PJ, Ul-Hasan S, van der Hooft JJJ, Vargas F, Vázquez-Baeza Y, Vogtmann E, von Hippel M, Walters W, Wan Y, Wang M, Warren J, Weber KC, Williamson CHD, Willis AD, Xu ZZ, Zaneveld JR, Zhang Y, Zhu Q, Knight R, Caporaso JG. 2019. Reproducible, interactive, scalable and extensible microbiome data science using QIIME 2. Nat Biotechnol 37:852–857.

78. Callahan BJ, McMurdie PJ, Rosen MJ, Han AW, Johnson AJA, Holmes SP. 2016. DADA2: High-resolution sample inference from Illumina amplicon data. Nat Methods 13:581–583.

79. Quast C, Pruesse E, Yilmaz P, Gerken J, Schweer T, Yarza P, Peplies J, Glöckner FO. 2013. The SILVA ribosomal RNA gene database project: Improved data processing and web-based tools. Nucleic Acids Res 41:590–596.

80. Bokulich NA, Kaehler BD, Rideout JR, Dillon M, Bolyen E, Knight R, Huttley GA, Gregory Caporaso J. 2018. Optimizing taxonomic classification of marker-gene amplicon sequences with QIIME 2's q2-feature-classifier plugin. Microbiome 6:1–17.

81. Barott KL, Rodriguez-Brito B, Janouškovec J, Marhaver KL, Smith JE, Keeling P, Rohwer FL. 2011. Microbial diversity associated with four functional groups of benthic reef algae and the reef-building coral Montastraea annularis. Environ Microbiol 13:1192–1204.

82. Singer JR, Blosser EG, Zindl CL, Silberger DJ, Conlan S, Laufer VA, DiToro D, Deming C, Kumar R, Morrow CD, Segre JA, Gray MJ, Randolph DA, Weaver CT. 2019. Preventing dysbiosis of the neonatal mouse intestinal microbiome protects against late-onset sepsis. Nat Med 25:1772–1782.

83. Northrop AC, Brooks RK, Ellison AM, Gotelli NJ, Ballif BA. 2017. Environmental proteomics reveals taxonomic and functional changes in an enriched aquatic ecosystem. Ecosphere 8.

84. Beghini F, Renson A, Zolnik CP, Geistlinger L, Usyk M, Moody TU, Thorpe L, Dowd JB, Burk R, Segata N, Jones HE, Waldron L. 2019. Tobacco exposure associated with oral microbiota oxygen utilization in the New York City Health and Nutrition Examination Study. Ann Epidemiol 34:18-25.e3.

85. Suzuki TA, Martins FM, Nachman MW. 2019. Altitudinal variation of the gut microbiota in wild house mice. Mol Ecol 28:2378–2390.

86. Yu P, Zaleski A, Li Q, He Y, Mapili K, Pruden A, Alvarez PJJ, Stadler LB. 2018. Elevated Levels of Pathogenic Indicator Bacteria and Antibiotic Resistance Genes after Hurricane Harvey's Flooding in Houston. Environ Sci Technol Lett 5:481–486.

TABLE AND FIGURE LEGENDS

Table 1. Summary of sample collections from two reef sponge species at the East Bank (EB) and West Bank (WB) of the Flower Garden Banks National Marine Sanctuary (northwest Gulf of Mexico) and amplicon sequencing results of the V4 region of the 16S rRNA gene from sponge-associated bacterial communities. Richness (Observed ASVs^) and diversity (Shannon H') were calculated from rarefied ASV tables. Data are presented as mean ± (sem).

					Sequence Analysis Summary		
Species	Date	Site	Health Status	N	High Quality Sequences#	Observed ASVs^	Shannon H'
Various species	Jul. 2016	EB	Dead*	8	64,105 (8,903)	311 (32)	5.37 (0.36)
Agelas clathrodes	Aug. 2016	EB	Diseased	4	80,913 (6,339)	471 (83)	5.51 (0.93)
		EB	Healthy	8	86,833 (5,458)	231 (16)	5.32 (0.09)
		WB	Healthy	5	60,978 (8,011)	192 (27)	4.70 (0.34)
	Oct. 2017	EB	Healthy	9	24,540 (2,378)	102 (8)	3.93 (0.29)
		WB	Healthy	8	23,578 (1,175)	108 (7)	4.67 (0.34)
	Oct. 2018	EB	Healthy	10	26,992 (1,075)	155 (5)	5.69 (0.07)
		WB	Healthy	10	27,039 (1,041)	146 (4)	5.47 (0.11)
Xestospongia muta	Aug. 2016	EB	Diseased	5	60,897 (3,783)	386 (33)	6.27 (0.21)
		EB	Healthy	2	98,460 (1,837)	350 (67)	6.35 (0.67)
		WB	Healthy	3	96,329 (9,211)	254 (49)	5.17 (0.93)
	Sept. 2017	EB	Healthy	9	31,687 (4,441)	247 (16)	6.26 (0.16)
	Oct. 2017	EB	Healthy	2	26,539 (1,573)	249 (11)	6.91 (0.08)
		WB	Healthy	3	26,907 (1,589)	191 (31)	5.63 (0.67)
	Oct. 2018	EB	Healthy	10	28,101 (2,507)	201 (10)	6.25 (0.13)
		WB	Healthy	10	27,559 (1,680)	194 (11)	6.07 (0.16)

*samples collected from a variety of dead invertebrate tissue

#quality filtering included removal of low quality, short, Mitochondrial, Chloroplast, and Unassigned reads

^Amplicon Sequence Variants (ASVs) after rarefying to equal depth (12,000 reads)

Table 2. Bacterial taxaunique to both visually healthy *X. muta* and *A. clathrodes*-associated bacterial communities following the Tax Day flooding event (Aug. 2016) according to Indicator Species Analysis. Analysis was conducted on each sponge species individually. No ASVs* associated with the Oct. 2017 (1-month post-Hurricane Harvey) flooding were present in both *X. muta* and *A. clathrodes*-associated bacterial communities. No *X. muta*-associated ASVs were indicative of both flooding events (Aug. 2016 and Sept. 2017).

Date	ASV* ID	Taxonomy (Phylum_Class_Family_Genus)	Host	Indicator Value	P-value
Aug. 2016	ccd8d5e31ad9bfa58066251ea1138225	Bacteroidota_Bacteroidia_unclassifed Flavobacteriaceae	*X. muta*	0.466	0.026
			A. clathrodes	0.428	0.005
	64805be33440e427c18e31e0d5e6094b	Bacteroidota_Bacteroidia_Saprospiraceae_Phaeodactylibacter	*X. muta*	0.545	0.026
			A. clathrodes	0.436	0.001
	f3a2c825531c54cfc115b7b818561953	Bacteroidota_Bacteroidia_uncultured Saprospiraceae	*X. muta*	0.498	0.026
			A. clathrodes	0.397	0.003
	6a1e4b41f741b4fd1a7adac461779ab7	Cyanobacteria_Cyanobacteriia_Cyanobiaceae_Prochlorococcus	*X. muta*	0.514	0.027
			A. clathrodes	0.535	0.001
	0261a50c7edb68abf5e65bb5094ce011	Desulfobacterota_Desulfovibrionia_Desulfovibrionaceae_Desulfovibrio	*X. muta*	0.471	0.026
			A. clathrodes	0.534	0.000
	e51947121c608cf15031596f9d0c09eb	Desulfobacterota_Desulfovibrionia_Desulfovibrionaceae_Desulfovibrio	*X. muta*	0.453	0.026
			A. clathrodes	0.402	0.000
	e09f2d58d292332880fe9e37607469e1	Desulfobacterota_Desulfovibrionia_Desulfovibrionaceae_Halodesulfovibrio	*X. muta*	0.819	0.000
			A. clathrodes	0.393	0.000
	e4a5985be454d1e8a3d50a2ab6ea7a8b	Desulfobacterota_Desulfovibrionia_Desulfovibrionaceae_Halodesulfovibrio	*X. muta*	0.576	0.002
			A. clathrodes	0.371	0.000
	eb46361ce52904349aabf94a3ad30512	Firmicutes_Clostridia_uncultured Clostridiaceae	*X. muta*	0.511	0.026
			A. clathrodes	0.332	0.000
	5546361caf3e42e50fb56d85a11571f2	Proteobacteria_Alphaproteobacteria_Clade I_Clade Ia	*X. muta*	0.529	0.022
			A. clathrodes	0.455	0.002
	f2335497138a785fb4288dfcf64a56c0	Proteobacteria_Gammaproteobacteria_Halieaceae_OM60(NOR5) clade	*X. muta*	0.565	0.026
			A. clathrodes	0.418	0.003
	2ef8937fcfef105310d9aae9f65c08ab	Proteobacteria_Gammaproteobacteria_Kangiellaceae_Aliikangiella	*X. muta*	0.545	0.026
			A. clathrodes	0.411	0.000
	9442980515ce7f911bb4cc9c372db4e8	Proteobacteria_Gammaproteobacteria_unclasified SAR86 clade	*X. muta*	0.782	0.000
			A. clathrodes	0.595	0.000
	9ec997c700d09a502a482a43b707b85c	Proteobacteria_Gammaproteobacteria_unclassified SAR86 clade	*X. muta*	0.696	0.002
			A. clathrodes	0.473	0.000
	b47b6e5813cfd4b7690b522531f10aa4	Proteobacteria_Gammaproteobacteria_Thioglobaceae_SUP05 cluster	*X. muta*	0.873	0.000
			A. clathrodes	0.376	0.015

*Amplicon Sequence Variants

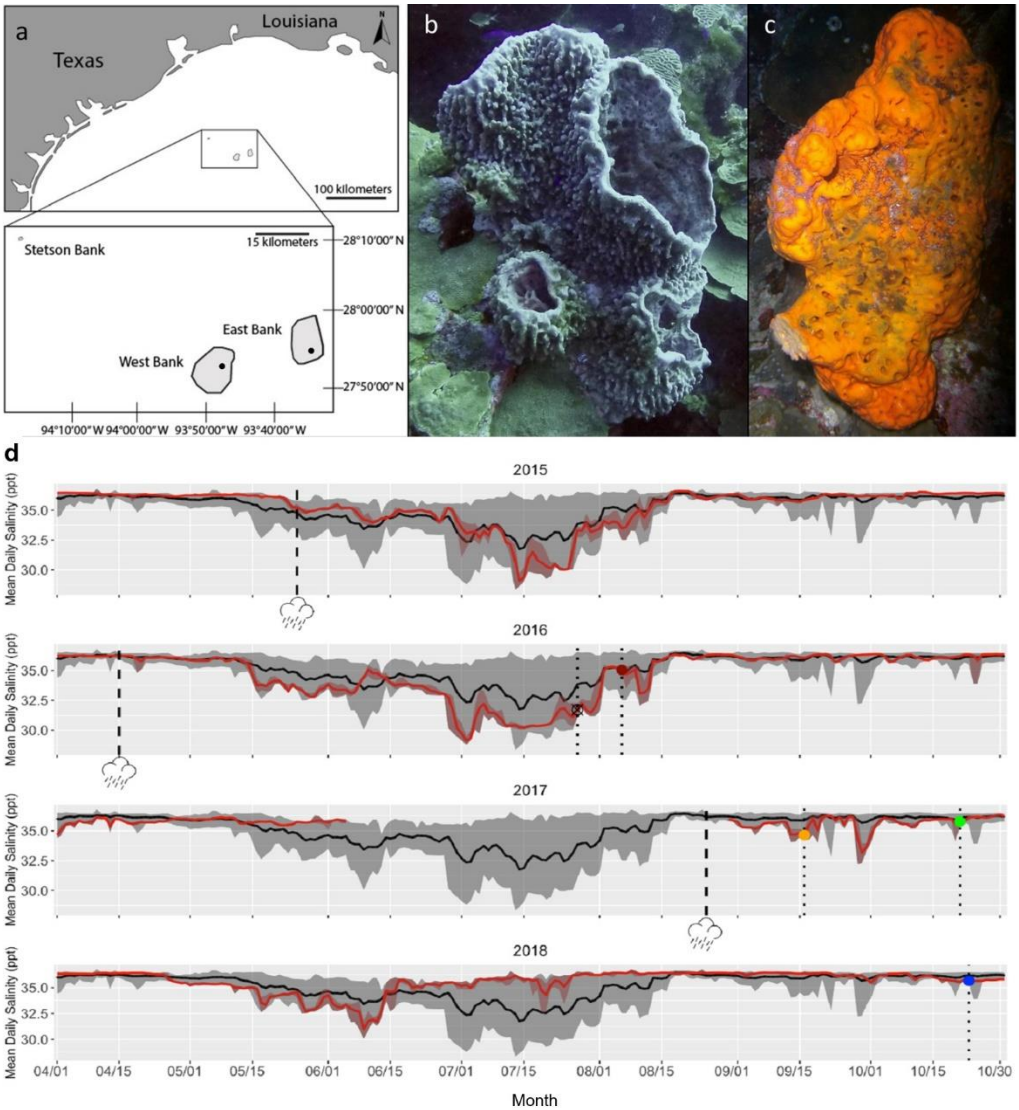

Figure 1. **Summary of study site, host taxa and local abiotic conditions associated with this study.** A) Map of Flower Garden Banks National Marine Sanctuary (northwest Gulf of Mexico) with sites of sponge collection indicated as black dots; B) Representative *Xestospongia muta* sponge; C) Representative *Agelas clathrodes* sponge; D) Surface Salinity (ppt) at buoy V spanning the months April through October in which sampling occurred for this study. Black lines represent daily means from 2013–2018 and grey shaded areas encompass minimum and maximum values from 2013–2018. Red lines represent daily means for 2015, 2016, 2017, and 2018, individually. Dashed lines with storm icon represent dates of terrestrial flooding. Dotted lines with symbols represent mean daily values on the date of each sample collection: black circle = 27 July 2016, dark red circle = 6 August 2016, orange circle = 16 September 2017, green circle = 21 October 2017, and blue circle = 23 October 2018.

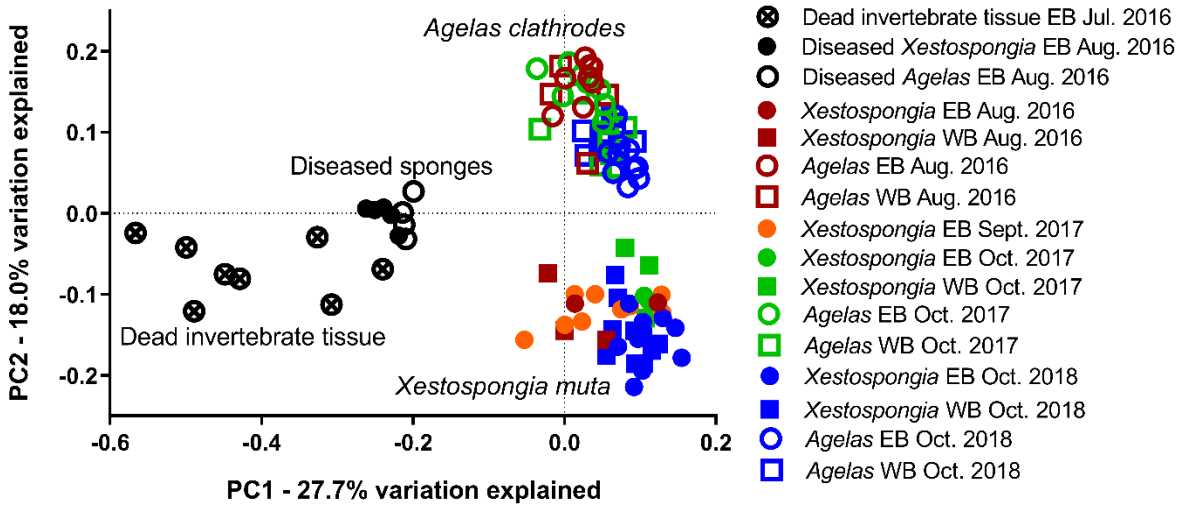

Figure 2. Principle Coordinate Analysis of the weighted UniFrac distance matrix for bacterial communities analyzed in this study. Empty symbols = *Agelas clathrodes* samples; filled symbols = *Xestospongia muta* samples. Black symbols = samples from dead invertebrate tissue and diseased sponges during (July 2016) and immediately after (August 2016) the mortality event; Red symbols = visually healthy sponge samples collected immediately after the 2016 mortality event. Orange symbols = samples collected immediately following Hurricane Harvey (Sept. 2017) from visually healthy sponges; Green symbols = samples collected one month following Hurricane Harvey (Oct. 2017) from visually healthy sponges. Blue symbols = samples collected in a no-flood (baseline) year from visually healthy sponges (Oct. 2018). Circles = samples collected from East Bank (EB); squares = samples collected from West Bank (WB) of the Flower Garden Banks National Marine Sanctuary (northern Gulf of Mexico).

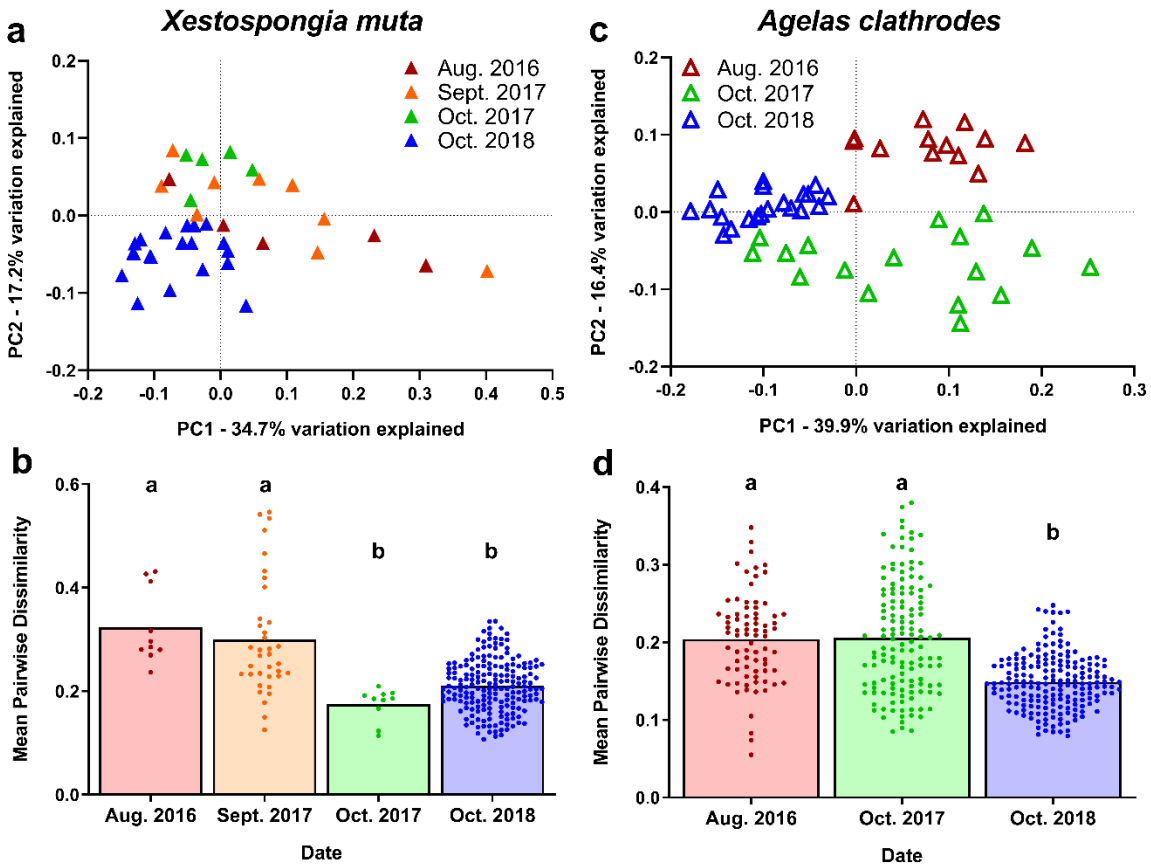

Figure 3. Sponge-associated bacterial communities differed in composition and variability following extreme storm-derived floods. Principle Coordinate Analysis of the weighted UniFrac distance matrices for visually healthy a) *Xestospongia muta* and c) *Agelas clathrodes* bacterial communities. Mean (with individual value dots) pairwise dissimilarity values for b) *X. muta* and d) *A. clathrodes*. Red = August 2016. Orange = September 2017; Green = October 2017. Blue = October 2018 associated with no flooding stress. Bars represent mean (± sem). Within a species, bars that do not share a letter are significantly different based on Kruskal-Wallis test with Dunn's multiple comparisons ($p < 0.05$).

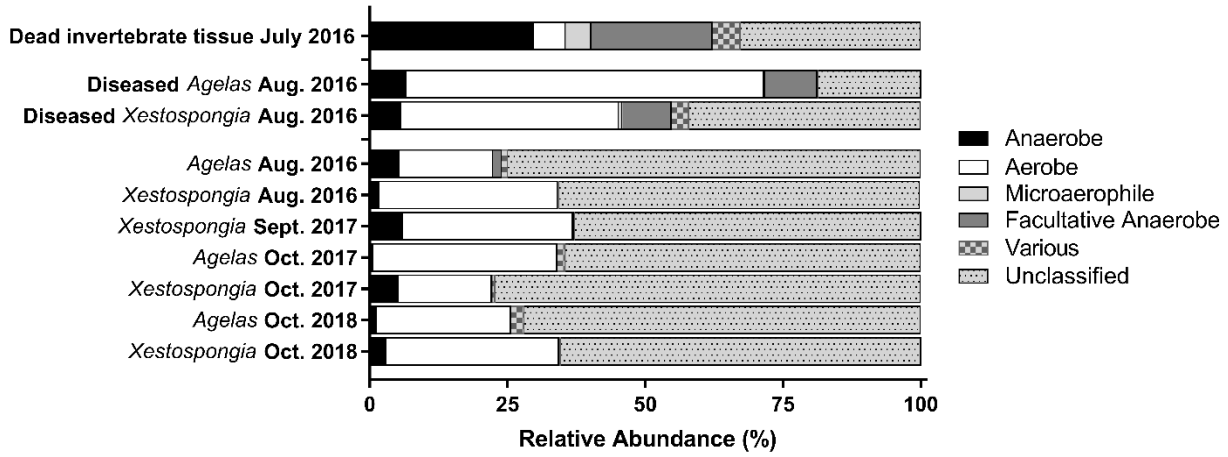

Figure 4. Percent abundance of bacterial sequences classified by oxygen requirement, for dead invertebrate tissue samples (July 2016), diseased sponges (August 2016), and visually healthy sponges (2016, 2017, 2018). Flood events occurred in the region in 2016 and 2017, but not in 2018. Bacterial taxonomy was assigned using the SILVA v138 database, and oxygen requirements of each Genus were classified using Bergey's Manual of Systematics of Archaea and Bacteria (35), the Integrated Microbial Genomes database (IMG; https://img.jgi.doe.gov/), and the eLibrary of Microbial Systematics and Genomics (eLMG; https://www.biosino.org/elmsg/index). Genera with more than one type of oxygen requirement were categorized as 'Various', and taxonomic assignments not assigned to the level of Genus were categorized as "Unclassified"

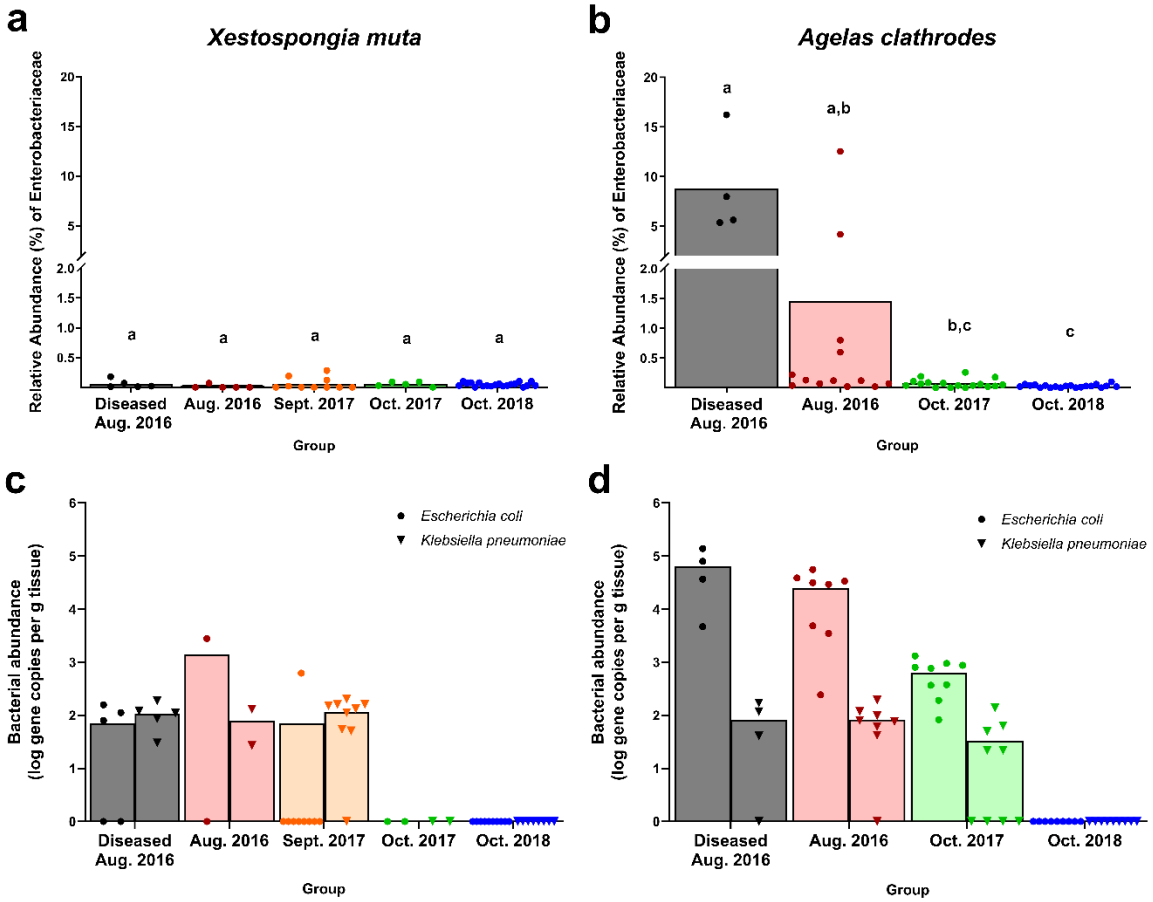

Figure 5. Relative abundance of sequences in the Family Enterobacteriaceae (a,b) and to specific human pathogens (*Escherichia coli* and *Klebsiella pneumoniae)* (c,d) across sites and years. Data in (a,b) are based on Illumina MiSeq amplicon sequencing of the V4 region of the bacterial 16S rRNA gene. Data in (c,d) are quantitative PCR amplification of the bacterial *ybbW* and *phoE* genes for *E. coli* and *K. pneumoniae*, respectively. All data are presented as mean with individual value dots. Black bars = affected sponges in 2016; red bars = healthy sponges in 2017; green bars = healthy sponges in 2017; blue bars = healthy sponges in 2018 (no flood, baseline year). Groups that share a letter (in a, b) are not significantly different based on Kruskal-Wallis with Dunn's multiple comparisons across groups within a species. ND = not detected.